Application of Second-Order-Accurate Total Variation Diminishing (TVD) Schemes to the Euler Equations in General Geometries

H. C. Yee and P. Kutler

(NASA-TM-85845) APPLICATION OF SECOND-ORDER-ACCURATE TOTAL VARIATION DIMINISHING (TVD) SCHEMES TO THE EULER EQUATIONS IN GENERAL GEOMETRIES (NASA) 21 p HC A02/MF A01 CSCL 12A G3/64

N83-35710

Unclas
42130

August 1983

ERRATA

NASA Technical Memorandum 85845

Application of Second-Order-Accurate Total Variation Diminishing (TVD) Schemes to the Euler Equations in General Geometries

H.C. Yee and P. Kutler

August 1983

Page 3: Equations (3a) and (3b) should be

$$\hat{A} = \xi_x A + \xi_y B$$
$$\hat{B} = \eta_x A + \eta_y B$$

Page 4: Equation (5a), the 4th column of the matrix should be _____

$$\begin{bmatrix} 0 \\ k_2 \\ -k_1 \\ -k_1 v + k_2 u \end{bmatrix}$$

Page 4: Equation (5b) should be

$$k_1 = \xi_x / k_\xi, \qquad k_2 = \xi_y / k_\xi$$

Page 6: The right hand sides of equations (8e) and (8f) should be the individual variables divided by the corresponding Jacobians.

Pages 17-18: All the numerical results were obtained using the correct formulae.

Application of Second-Order-Accurate Total Variation Diminishing (TVD) Schemes to the Euler Equations in General Geometries

H. C. Yee
P. Kutler, Ames Research Center, Moffett Field, California

NASA
National Aeronautics and
Space Administration

Ames Research Center
Moffett Field, California 94035

Application of Second-Order-Accurate Total Variation Diminishing (TVD) Schemes to the Euler Equations in General Geometries

H.C. Yee† and P. Kutler‡

NASA Ames Research Center, Moffett Field, CA., 94035

Abstract. A one-parameter family of explicit and implicit second-order-accurate, entropy satisfying, total variation diminishing (TVD) schemes has been developed by Harten. These TVD schemes have the property of not generating spurious oscillations for one-dimensional nonlinear scalar hyperbolic conservation laws and constant coefficient hyperbolic systems. Application of these methods to one- and two-dimensional fluid flows containing shocks (in Cartesian coordinates) yields highly accurate nonoscillatory numerical solutions. The goal of this work is to extend these methods to the multidimensional Euler equations in generalized coordinate systems. Some numerical results of shock waves impinging on cylindrical bodies are compared with MacCormack's method.

§1. Motivation and Objective

Several techniques for the construction of nonlinear, second-order-accurate, high-resolution, entropy satisfying schemes for hyperbolic conservation laws have been developed in recent years. See, for example, van Leer [1], Colella and Woodward [2], Harten [3,4], Roe [5] and Osher [6]. We can also view these schemes as shock-capturing algorithms based on either an exact or approximate Riemann solver. From the standpoint of numerical analysis, these schemes are TVD for one-dimensional nonlinear scalar hyperbolic conservation laws and for one-dimensional constant coefficient hyperbolic systems. In [4], Harten introduced the notion of TVD schemes. Entropy satisfying TVD schemes have the property that they do not generate spurious oscillations and that the weak solutions are physical ones. The goal of constructing these highly nonlinear schemes is to simulate complex flow fields more accurately (i.e., to construct schemes that are stable in a strong nonlinear sense). TVD schemes are usually rather complicated to use compared

†Research Scientist, Computational Fluid Dynamics Branch.
‡Chief, Applied Computational Aerodynamics Branch.

with the conventional shock-capturing methods such as variants of the Lax-Wendroff scheme. The complexity of these schemes has inhibited their application to complicated flow geometries in the past.

Application of Harten's explicit and implicit methods to standard one- and two-dimensional transient and steady-state gas-dynamic test problems in Cartesian coordinates was examined by Harten [3] and Yee et al. [7-9]. In both one and two dimensions, accurate solutions containing shocks and contact discontinuities were obtained.

The objective of this report is to extend Harten's TVD method to generalized coordinate systems, and to test the method on a two-dimensional problem of a moving shock wave impinging on a cylinder. The numerical results are compared with MacCormack's explicit method. From here on, we refer to this method as the TVD scheme.

A description of the TVD algorithms in Cartesian coordinates can be found in reference [9]. A description of this method for two-dimensional Euler equations in generalized coordinate systems will be discussed in the next section. Some results on the shock wave-cylinder interaction are presented in section 3.

§2. Extension of an Explicit TVD Scheme for the Euler Equations in Generalized Coordinate Systems

Here we assume the reader is either familar with the development and properties of explicit and implicit TVD schemes, or will consult the appropriate references [3,4,7-9]. A brief description of these methods and a detailed implementation of these methods for one- and two-dimensional Euler equations of gas dynamics can be found in reference [9]. To avoid extra notation, a particular form of the explicit TVD scheme in [3] is extended to generalized coordinates. Generalization of the implicit TVD scheme to arbitrary geometries follows the same procedure.

§2.1 The Euler Equations

In two spatial dimensions, the Euler equations of gas dynamics can be written in the conservative form as

$$\frac{\partial Q}{\partial t} + \frac{\partial F(Q)}{\partial x} + \frac{\partial G(Q)}{\partial y} = 0 \tag{1a}$$

where

$$Q = \begin{bmatrix} \rho \\ m \\ n \\ e \end{bmatrix}, \quad F = \begin{bmatrix} m \\ m^2/\rho + p \\ mv \\ (e+p)m/\rho \end{bmatrix}, \quad G = \begin{bmatrix} n \\ nu \\ n^2/\rho + p \\ (e+p)n/\rho \end{bmatrix} \tag{1b}$$

with $m = \rho u$ and $n = \rho v$. The primitive variables are the density ρ, the velocity components u and v, and the pressure p. The total energy per unit volume e, is related to p by the equation of state for a perfect gas

$$p = (\gamma - 1)\left[e - \frac{(m^2 + n^2)}{2\rho}\right] \tag{1c}$$

where γ is the ratio of specific heats.

A generalized coordinate transformation of the form $\xi = \xi(x, y)$ and $\eta = \eta(x, y)$ which maintains the strong conservation law form of equation (1) is given by

$$\frac{\partial \hat{Q}}{\partial t} + \frac{\partial F(\hat{Q})}{\partial \xi} + \frac{\partial G(\hat{Q})}{\partial \eta} = 0 \tag{2}$$

where $\hat{Q} = Q/J$, $\hat{F} = (\xi_x F + \xi_y G)/J$, $\hat{G} = (\eta_x F + \eta_y G)/J$, and $J = \xi_x \eta_y - \xi_y \eta_x$, the Jacobian of transformation. Let $A = \partial F/\partial Q$ and $B = \partial G/\partial Q$; then the Jacobian $\hat{A}$ and $\hat{B}$ of $\hat{F}$ and $\hat{G}$ can be written as

$$\hat{A} = (\xi_x A + \xi_y B)/J \tag{3a}$$

$$\hat{B} = (\eta_x A + \eta_y B)/J \tag{3b}$$

Let c be the local speed of sound; the eigenvalues of $\hat{A}$ are

$$(a_\xi^1, a_\xi^2, a_\xi^3, a_\xi^4) = (\hat{U} - k_\xi c, \quad \hat{U}, \quad \hat{U} + k_\xi c, \quad \hat{U}) \tag{4a}$$

where $\hat{U} = (\xi_x u + \xi_y v)$ and $k_\xi = \sqrt{\xi_x^2 + \xi_y^2}$. The eigenvalues of $\hat{B}$ are

$$(a_\eta^1, a_\eta^2, a_\eta^3, a_\eta^4) = (\hat{V} - k_\eta c, \quad \hat{V}, \quad \hat{V} + k_\eta c, \quad \hat{V}) \tag{4b}$$

where $\hat{V} = (\eta_x u + \eta_y v)$ and $k_\eta = \sqrt{\eta_x^2 + \eta_y^2}$

Furthermore, let $R_\xi = (R_\xi^1, R_\xi^2, R_\xi^3, R_\xi^4)$ and $R_\eta = (R_\eta^1, R_\eta^2, R_\eta^3, R_\eta^4)$ be the matrices whose columns are eigenvectors of $\hat{A}$ and $\hat{B}$. Let R_ξ^{-1} and R_η^{-1} be the inverses of R_ξ and R_η. A form of R_ξ and R_ξ^{-1} can be written as

$$R_\xi = \begin{bmatrix} 1 & 1 & 1 & 0 \\ u - k_1 c & u & u + k_1 c & -k_2 \\ v - k_2 c & v & v + k_2 c & k_1 \\ H - k_1 u c - k_2 v c & (u^2 + v^2)/2 & H + k_1 u c + k_2 v c & k_1 v - k_2 u \end{bmatrix} \tag{5a}$$

where

$$k_1 = \xi_x, \qquad k_2 = \xi_y \tag{5b}$$

$$H = \frac{c^2}{\gamma - 1} + \frac{u^2 + v^2}{2} \tag{5c}$$

and

$$R_\xi^{-1} = \begin{bmatrix} \frac{1}{2}(b_1 + k_1 u/c + k_2 v/c) & \frac{1}{2}(-b_2 u - k_1/c) & \frac{1}{2}(-b_2 v - k_2/c) & \frac{1}{2} b_2 \\ 1 - b_1 & b_2 u & b_2 v & -b_2 \\ \frac{1}{2}(b_1 - k_1 u/c - k_2 v/c) & \frac{1}{2}(-b_2 u + k_1/c) & \frac{1}{2}(-b_2 v + k_2/c) & \frac{1}{2} b_2 \\ -k_2 u + k_1 v & k_2 & -k_1 & 0 \end{bmatrix} \tag{6a}$$

with

$$b_1 = b_2 \frac{(u^2 + v^2)}{2} \tag{6b}$$

$$b_2 = \frac{\gamma - 1}{c^2} \tag{6c}$$

Let the grid spacing be denoted by $\Delta\xi$ and $\Delta\eta$ such that $\xi = j\Delta\xi$ and $\eta = k\Delta\eta$. Denote $\hat{Q}_{j+1/2,k}$ as some symmetric average of $\hat{Q}_{j,k}$ and $\hat{Q}_{j+1,k}$ (for example, the Roe's average [10]). Let $a^l_{j+1/2}$, $R_{j+1/2}$, $R^{-1}_{j+1/2}$ denote the quantities of a^l_ξ, R_ξ, R^{-1}_ξ related to $\hat{A}$ evaluated at $\hat{Q}_{j+1/2,k}$. Similarly, let $a^l_{k+1/2}$, $R_{k+1/2}$, $R^{-1}_{k+1/2}$ denote the quantities of a^l_η, R_η, R^{-1}_η related to $\hat{B}$ evaluated at $\hat{Q}_{j,k+1/2}$.

We define

$$\alpha_{j+1/2} = R^{-1}_{j+1/2}(\hat{Q}_{j+1,k} - \hat{Q}_{j,k}) \tag{7a}$$

as the component of $(\hat{Q}_{j+1,k} - \hat{Q}_{j,k})$ (omitting the k index) in the locally l-th characteristic ξ-direction [9]. Denote

$$\alpha_{k+1/2} = R^{-1}_{k+1/2}(\hat{Q}_{j,k+1} - \hat{Q}_{j,k}) \tag{7b}$$

as the component of $(\hat{Q}_{j,k+1} - \hat{Q}_{j,k})$ (omitting the j index) in the locally l-th characteristic η-direction. The vector α of equation (7a) can be written as

$$\begin{bmatrix} \alpha^1_{j+1/2} \\ \alpha^2_{j+1/2} \\ \alpha^3_{j+1/2} \\ \alpha^4_{j+1/2} \end{bmatrix} = \begin{bmatrix} (aa - bb)/2 \\ \Delta_{j+1/2}\rho - aa \\ (aa + bb)/2 \\ cc \end{bmatrix} \tag{8a}$$

where

$$aa = \frac{\gamma - 1}{c^2_{j+1/2}}\left[\Delta_{j+1/2}e + \frac{u^2_{j+1/2} + v^2_{j+1/2}}{2}\Delta_{j+1/2}\rho - u_{j+1/2}\Delta_{j+1/2}m - v_{j+1/2}\Delta_{j+1/2}n\right] \tag{8b}$$

$$bb = \frac{1}{c_{j+1/2}}\left[k_1\Delta_{j+1/2}m - (k_1u_{j+1/2} + k_2v_{j+1/2})\Delta_{j+1/2}\rho + k_2\Delta_{j+1/2}n\right] \tag{8c}$$

$$cc = -k_1\Delta_{j+1/2}n - (k_2u_{j+1/2} - k_1v_{j+1/2})\Delta_{j+1/2}\rho + k_2\Delta_{j+1/2}m \tag{8d}$$

with

$$\Delta_{j+1/2}\rho = \rho_{j+1,k} - \rho_{j,k}, \qquad \Delta_{j+1/2}m = m_{j+1,k} - m_{j,k} \tag{8e}$$

and

$$\Delta_{j+1/2}n = n_{j+1,k} - n_{j,k}, \qquad \Delta_{j+1/2}e = e_{j+1,k} - e_{j,k} \tag{8f}$$

The simplest form for $\hat{Q}_{j+1/2,k}$ is

$$\hat{Q}_{j+1/2,k} = (\hat{Q}_{j+1,k} + \hat{Q}_{j,k})/2 \tag{9}$$

Roe's form of the averaging in the ξ-direction is:

$$u_{j+1/2,k} = \frac{\overline{D}u_{j+1,k} + u_{j,k}}{\overline{D}+1} \tag{10a}$$

$$v_{j+1/2,k} = \frac{\overline{D}v_{j+1,k} + v_{j,k}}{\overline{D}+1} \tag{10b}$$

$$H_{j+1/2,k} = \frac{\overline{D}H_{j+1,k} + H_{j,k}}{\overline{D}+1} \tag{10c}$$

$$c^2_{j+1/2,k} = (\gamma-1)\left[H_{j+1/2,k} - \frac{1}{2}(u^2_{j+1/2,k} + v^2_{j+1/2,k})\right] \tag{10d}$$

$$\overline{D} = \sqrt{\rho_{j+1,k}/\rho_{j,k}} \tag{10e}$$

$$H = \frac{\gamma p}{(\gamma-1)\rho} + \frac{1}{2}(u^2+v^2) \tag{10f}$$

Therefore to use Roe's averaging for the ξ-differencing, all one has to do is compute $u_{j+1/2,k}$, $v_{j+1/2,k}$, and $c_{j+1/2,k}$ in equations (4a), (5)-(6), (7a) and (8) by equation (10). Similarly, Roe's averaging can be obtained for $u_{j,k+1/2}$, $v_{j,k+1/2}$, and $c_{j,k+1/2}$. In the numerical experiments for the two-dimensional test problem, Roe's averaging is used.

§2.2 Algorithm of a TVD Method in Generalized Coordinates

Let $h = \Delta t$ be the time step; then a particular form of the explicit TVD method of [3] in generalized coordinates, when implemented by the method of fractional steps, can be written as follows:

$$\hat{Q}_{j,k}^{n+2} = L_\xi^{h/2} L_\eta^h L_\xi^h L_\eta^h L_\xi^{h/2} \hat{Q}_{j,k}^n \tag{11a}$$

where

$$\hat{Q}_{j,k}^* = \hat{Q}_{j,k}^n - \frac{\Delta t}{\Delta \xi}(\check{F}_{j+1/2,k}^n - \check{F}_{j-1/2,k}^n) = L_\xi^h \hat{Q}_{j,k}^n \tag{11b}$$

$$\hat{Q}_{j,k}^{n+1} = \hat{Q}_{j,k}^* - \frac{\Delta t}{\Delta \eta}(\check{G}_{j,k+1/2}^* - \check{G}_{j,k-1/2}^*) = L_\eta^h \hat{Q}_{j,k}^* \tag{11c}$$

Here

$$\check{F}_{j+1/2,k}^n = \frac{1}{2}\left[\hat{F}(\hat{Q}_{j,k}) + \hat{F}(\hat{Q}_{j+1,k})\right] + \frac{\Delta \xi}{2\Delta t}\sum_{l=1}^{4}\left[\kappa_{j+1/2}^l(\overrightarrow{g}_j^l + \overrightarrow{g}_{j+1}^l) - \phi(\nu_{j+1/2}^l + \gamma_{j+1/2}^l)\alpha_{j+1/2}^l\right]R_{j+1/2}^l \tag{11d}$$

and

$$\check{G}_{j,k+1/2}^n = \frac{1}{2}\left[\hat{G}(\hat{Q}_{j,k}) + \hat{G}(\hat{Q}_{j,k+1})\right] + \frac{\Delta \eta}{2\Delta t}\sum_{l=1}^{4}\left[\kappa_{k+1/2}^l(\overrightarrow{g}_k^l + \overrightarrow{g}_{k+1}^l) - \phi(\nu_{k+1/2}^l + \gamma_{k+1/2}^l)\alpha_{k+1/2}^l\right]R_{k+1/2}^l \tag{11e}$$

with

$$\kappa_{j+1/2}^l = [1 + \omega^l \max(\theta_j^l, \theta_{j+1}^l)]/8 \tag{11f}$$

$$\theta_j^l = \frac{|\alpha_{j+1/2}^l - \alpha_{j-1/2}^l|}{|\alpha_{j+1/2}^l| + |\alpha_{j-1/2}^l|} \tag{11g}$$

$$0 \le \omega^l \le 2 \tag{11h}$$

$$\bar{g}^l_j = S \cdot \max\left[0, \min(|\alpha^l_{j+1/2}|, S \cdot \alpha^l_{j-1/2})\right] \tag{11i}$$
$$S = \text{sign}(\alpha^l_{j+1/2})$$

$$\phi(\nu^l_{j+1/2} + \gamma^l_{j+1/2}) = (\nu^l_{j+1/2} + \gamma^l_{j+1/2})^2 + 1/4 \tag{11j}$$

$$\nu^l_{j+1/2} = \frac{\Delta t}{\Delta \xi} a^l_{j+1/2} \tag{11k}$$

and

$$\gamma^l_{j+1/2} = \kappa^l_{j+1/2} \begin{cases} (\bar{g}^l_{j+1} - \bar{g}^l_j)/\alpha^l_{j+1/2} & \alpha^l_{j+1/2} \neq 0 \\ 0 & \alpha^l_{j+1/2} = 0. \end{cases} \tag{11l}$$

We can define the variables of equation (11e) by simply replacing the subscripts j and $j+1/2$ in equations (11f)-(11l) by k and $k+1/2$. Extension of the implicit TVD scheme [4,9] to a generalized coordinate system follows the same procedure as described above.

In general, if one handles the intermediate boundary conditions correctly, one only needs to do the half steps in (11a) at the beginning and immediately before printout; i.e.,

$$\hat{Q}^{n+2}_{j,k} = L^{h/2}_\xi L^h_\eta L^h_\xi \ldots L^h_\eta L^{h/2}_\xi \hat{Q}^0_{j,k} \tag{12}$$

where $\hat{Q}^0_{j,k}$ is the initial condition.

§3. Numerical Result for the Shock Wave-Cylinder Interaction

A good test problem for assessing the capabilities of any shock-capturing scheme is the shock-diffraction problem; i.e., the computation of the unsteady flow field resulting from a planar moving shock wave striking an obstacle. In the present numerical experiment the diffraction process is determined over

a cylinder. The shock patterns at two instances in time t_1 and t_2 after initial impingement are sketched in Fig. 1.

When the incident shock first collides with the cylinder, regular reflection occurs at the shock impingement point. As the impingement point of the incident shock propagates around the body, the reflection process makes a transition from regular to Mach reflection. It should be pointed out that during the transition process, complex and double Mach reflection shock structures are possible. Their occurrence is dependent on the initial strength of the incident shock wave. For single Mach reflection, a triple point forms and the incident shock no longer touches the body. Emanating from the triple point are three waves: 1) a Mach stem which strikes the body perpendicularly, 2) a slip surface or shear layer which strikes the body and results in a vortical singularity (nodal point of streamlines), and 3) the reflected shock which propagates away from the body. In addition to the above flow field characteristics, a stagnation point (saddle point of streamlines) exists in the plane of symmetry, both forward and aft on the body.

The shock-diffraction problem contains most of the flow discontinuities possible with the Euler equations and is thus a good test for a numerical shock-capturing procedure. Both MacCormack's explicit method and the explicit TVD scheme were applied to the shock wave-cylinder interaction problem. For a fair comparision, the TVD scheme was implemented in an existing computer code [11] which also contained MacCormack's method, so that same initial conditions, boundary conditions and coordinate transformation were used. A cylindrical grid consisting of 50 points around the half-cylindrical (ξ-direction) body and 51 points between the body and outer boundary (η-direction) was used. The body radius is one and the distance from the body to the outer boundary is between 2 to 4 (depending on the incident shock Mach number). Rays from the coordinate system origin are spaced at equal angles with points uniformly placed in the radial direction between the body and the outer boundary (see Fig. 2).

§3.1 Initial and Boundary Conditions

Fig. 2 shows a schematic representation of the grid with its boundaries and initial conditions. The nodal points to the right of the planar moving shock are initialized to free stream values while those to the left are set equal to the post moving shock conditions. In the outer boundary, it is necessary to track the moving planar shock as a function of time along this boundary

surface.

At the planes of symmetry, the reflection principle is used; i.e., the pressure, density, and u-velocity component are treated as even functions across the plane of symmetry while the v-velocity component is treated as an odd function. The boundary condition at the surface of the cylinder must satisfy the tangency condition which requires that the velocity in the radial-direction be equal to zero at the body. Furthermore, for convenience, an image line of nodal points is considered which falls one mesh interval inside the body, so that the reflection principle can be applied.

§3.2 Numerical Result

MacCormack's method with a fourth-order dissipation term was run at a Courant (CFL) number of 0.6 for stability while the TVD method was operated at a Courant number of 0.9 for efficiency. The Courant number is a measure of the maximum permissible time step for a stable solution. The TVD method is insensitive to Courant number between 0.5 and 1. Both methods were run to approximately the same total time (100 steps for the MacCormack's method, 70 steps for the TVD method). The results in the form of pressure and density contour plots are shown in Fig. 3 at a time for which Mach reflection of the incident shock exists. The incident shock Mach number was 2. The results from MacCormack's method are shown in Figs. 3a and 3b. Those for the TVD method are shown in Figs. 3c and 3d. It can be seen that the TVD scheme results in a better defined flow field; i.e., "crisper" shocks and hardly any associated spurious oscillations. The slip surface which emanates from the triple point is smeared beyond recognition by both methods. It is, however, possible to observe the location on the body where the slip surface impinges (i.e., the vortical singularity). At this point, a local pressure minimum occurs, and the pressure contours, as a result, encircle it. This behavior can be observed in the pressure contour plot in the region to the left of the Mach stem at the body for the TVD scheme.

To test the shock-capturing capability of the TVD method at higher incident shock Mach numbers using the same grid size as before, cases were run at Mach numbers between 3 and 10. Figure 4 shows the pressure and density contour plots for the TVD scheme with an incident shock Mach number of 10 at a time when the incident shock was already passed the cylinder. For this case the Mach stem that extended from the triple point to the body

has struck the plane of symmetry and reflected from it. This will eventually make a transition to a Mach reflection just as it did at the body. The result shows that the TVD scheme is very stable and produces high resolution shock waves. The MacCormack method, on the other hand, was unstable under the same flow condition.

The TVD scheme requires approximately twice the CPU time per time step as MacCormack's method but results in enhanced numerical stability and solution accuracy.

§4 Concluding Remarks

The nonlinear, second-order accurate explicit TVD scheme in generalized coordinate systems has been applied to obtain transient solutions on the two-dimensional problem of a moving shock wave impinging on a cylinder. Fairly accurate solutions were obtained. Moreover, from numerical experiments, the scheme is stable in a strong nonlinear sense (e.g., the calculation with an incident shock Mach number of 10). The report is the first attempt to apply the TVD scheme to non-cartesian coordinates. It is preliminary in nature. Further research is underway on improving the resolution of discontinuities by the artificial compression method [12,13], and on improving the efficiency of computation by possibly using a large-time step (explicit method) approach [14].

ACKNOWLEGEMENT

The authors wish to thank Ami Harten for many enlightening suggestions. Special thanks to Robert Warming and Sukumar Chakravarthy for their valuable discussions throughout the course of this study.

REFERENCES

[1] B. van Leer, "Towards the Ultimate Conservative Difference Scheme. V. A Second-Order Sequel to Godunov's Method," J. Comp. Phys., Vol. 32, 1979, pp. 101-136.

[2] P. Colella and P.R. Woodward, "The Piecewise-Parabolic Method (PPM) for Gas-Dynamical Simulations," LBL report no. 14661, July 1982.

[3] A. Harten, "A High Resolution Scheme for the Computation of Weak Solutions of Hyperbolic Conservation Laws," J. Comp. Phys., Vol. 49, 1983, pp. 357-393.

[4] A. Harten, "On a Class of High Resolution Total-Variation-Stable Finite-Difference Schemes," to appear in SIAM J. Num. Anal.

[5] P.L. Roe, "Some Contributions to the Modelling of Discontinuous Flows," to appear in Proc. AMS-SIAM Summer Seminar on Large Scale Computations in Fluid Mechanics, Univ. of Calif. at San Diego, June 27-July 8 1983.

[6] S. Osher, "Shock Modeling in Transonic and Supersonic Flow," to appear in Recent Advances in Numerical Methods in Fluids, Vol. 4, Advances in Computational Transonics, W.G. Habashi Ed., Pineridge Press, 1984.

[7] H.C. Yee, R.F. Warming and A. Harten, "A High-Resolution Numerical Technique for Inviscid Gas-Dynamic Problems with Weak Solutions," Proc. Eighth International Conference on Numerical Methods in Fluid Dynamics, Aachen, West Germany, June 1982, Springer-Verlag.

[8] H.C. Yee, R.F. Warming and A. Harten, "On the Application and Extension of Harten's High-Resolution Scheme," NASA-TM-84256, June 1982.

[9] H.C. Yee, R.F. Warming and A. Harten, "Implicit Total Variation Diminishing (TVD) Schemes for Steady-State Calculations," AIAA Paper No. 83-1902, Proc. of the AIAA 6th Computational Fluid Dynamics Conference, Danvers, Mass., July, 1983.

[10] P.L. Roe, "Approximate Riemann Solvers, Parameter Vectors and Difference Schemes, " J. Comp. Phys., Vol. 43, 1981, pp. 357-372.

[11] P. Kutler, and A.R. Fernquist, "Computation of Blast Wave Encounter with Military Targets," Flow Simulations, Inc. Report No. 80-02, April 1980.

[12] A. Harten, "The Artificial Compression Method for Computation of Shocks and Contact Discontinuities. I. Single Conservation Laws," Comm. Pure Appl. Math., Vol. XXX, 1977, pp. 611-638.

[13] A. Harten, "The Artificial Compression Method for Computation of Shocks and Contact Discontinuities: III. Self-Adjusting Hybrid Schemes," Math. Comp., Vol. 32, No. 142, 1978, pp. 363-389.

[14] A. Harten, "On a Large Time-Step High Resolution Scheme," ICASE

Report No. 82-34, NASA Langley Research Center, Hampton Virginia, Nov. 15, 1982.

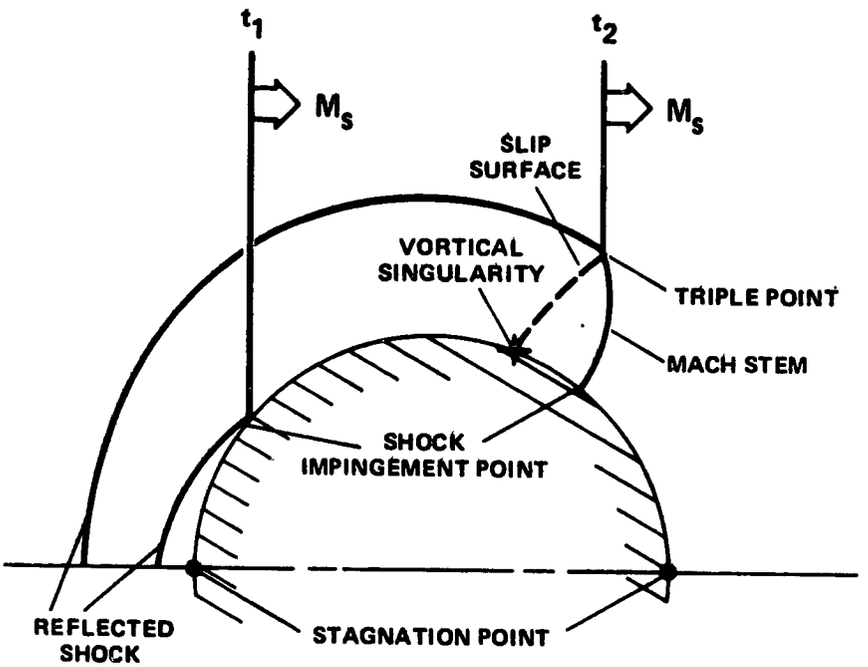

Fig. 1. Shock structure for shock diffraction over cylinder at two different times.

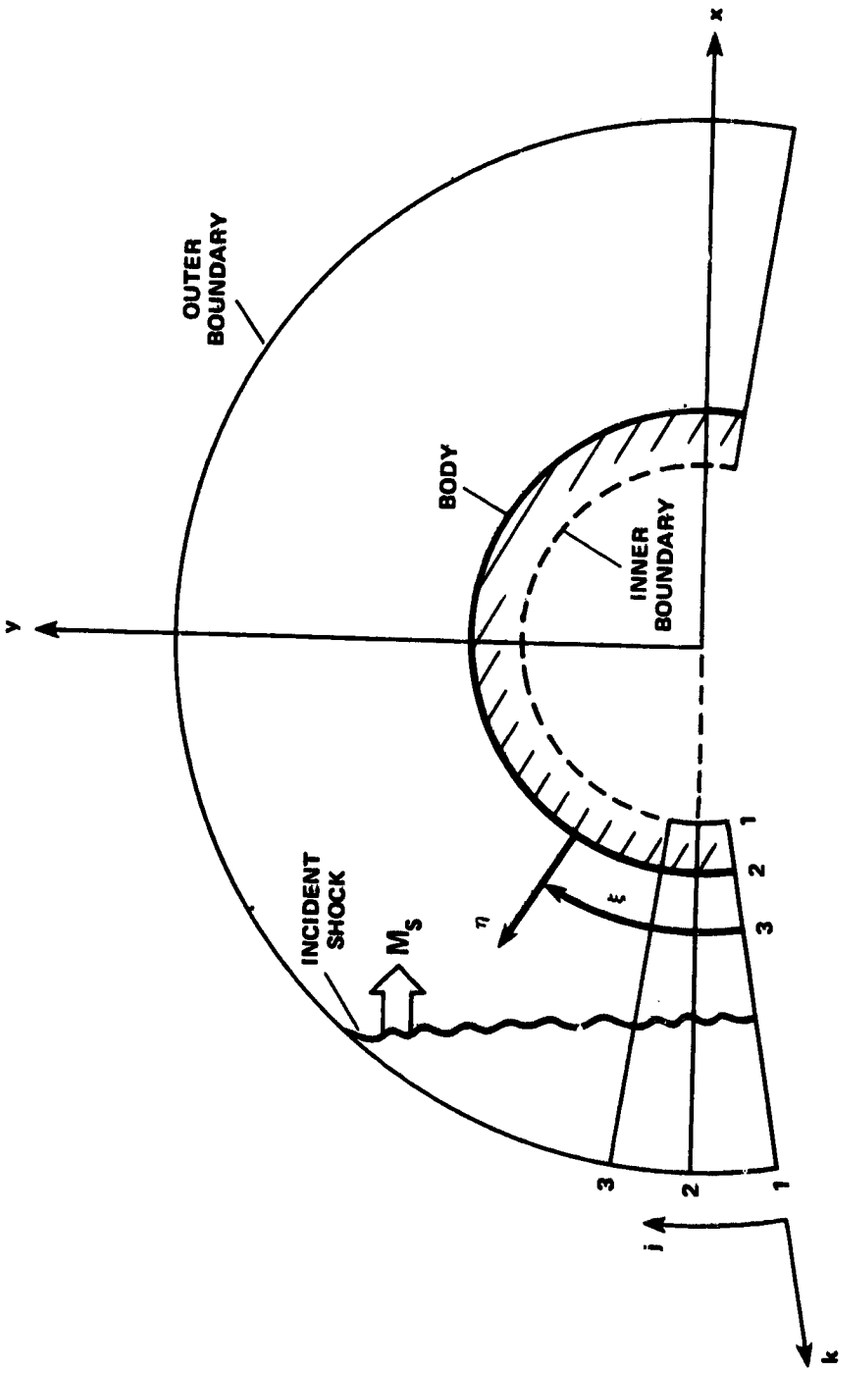

Fig. 2. Schematic of the computational grid.

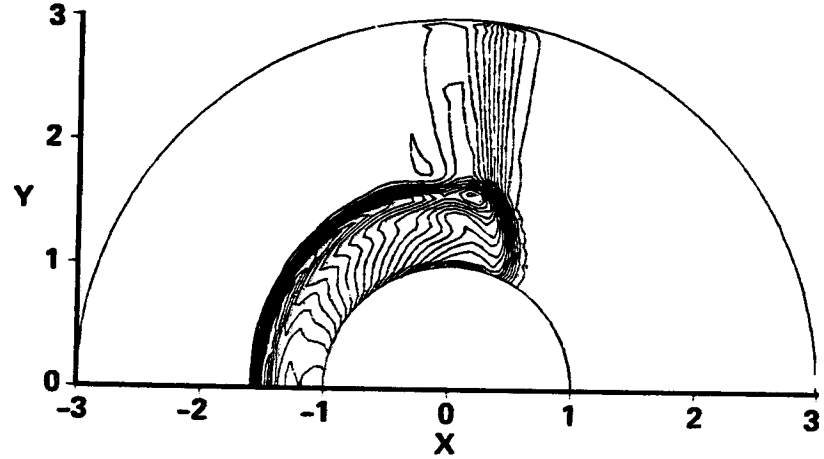

(a) Pressure contours: MacCormack's method.

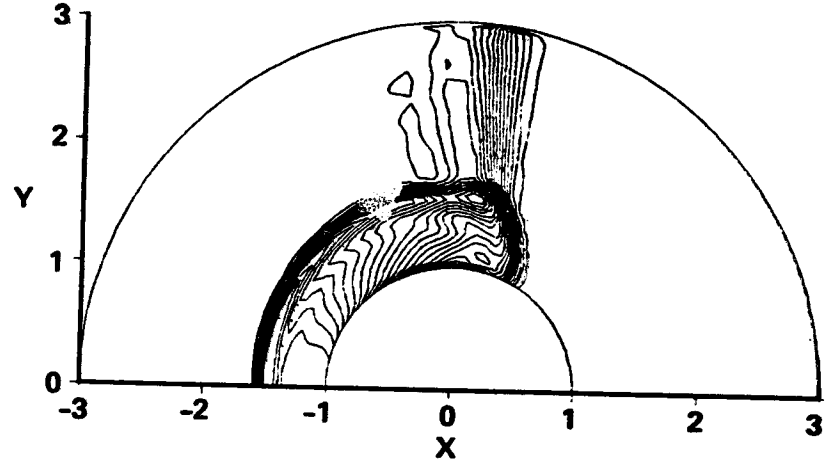

(b) Density contours: MacCormack's method.

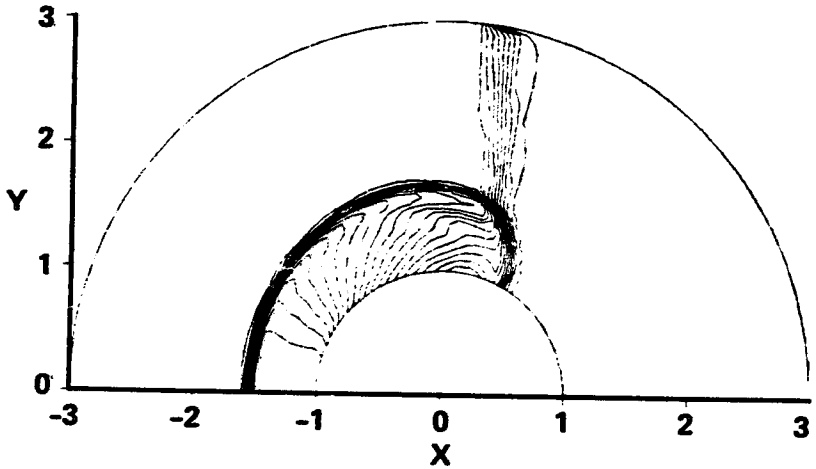

(c) Pressure contours: Explicit TVD method.

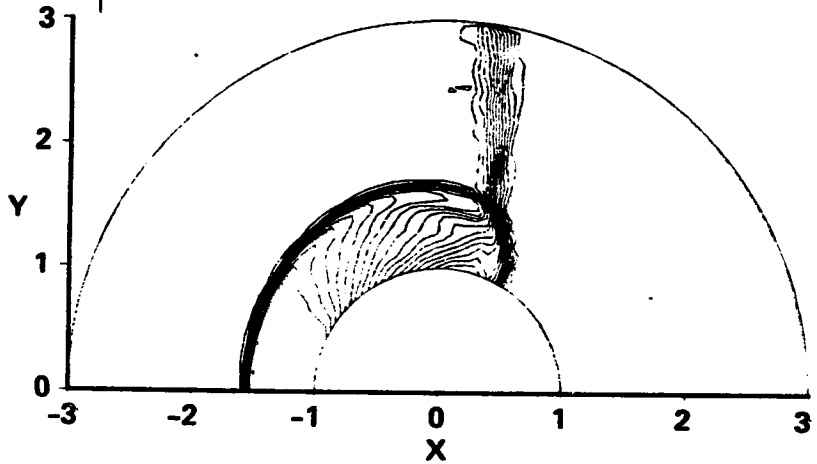

(d) Density contours: Explicit TVD method.

Fig. 3. Pressure and density contours for the shock-wave cylinder interaction. ($M_s = 2$).

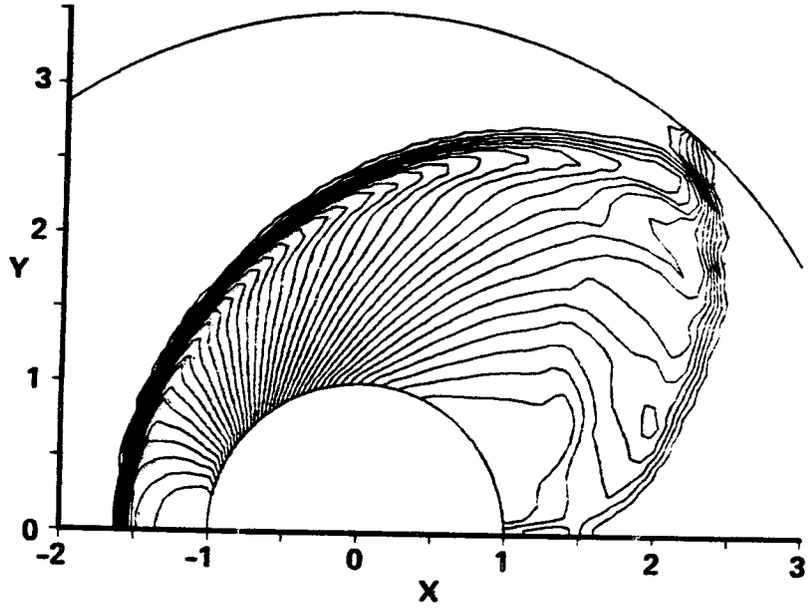

(a) Pressure contours: Explicit TVD method.

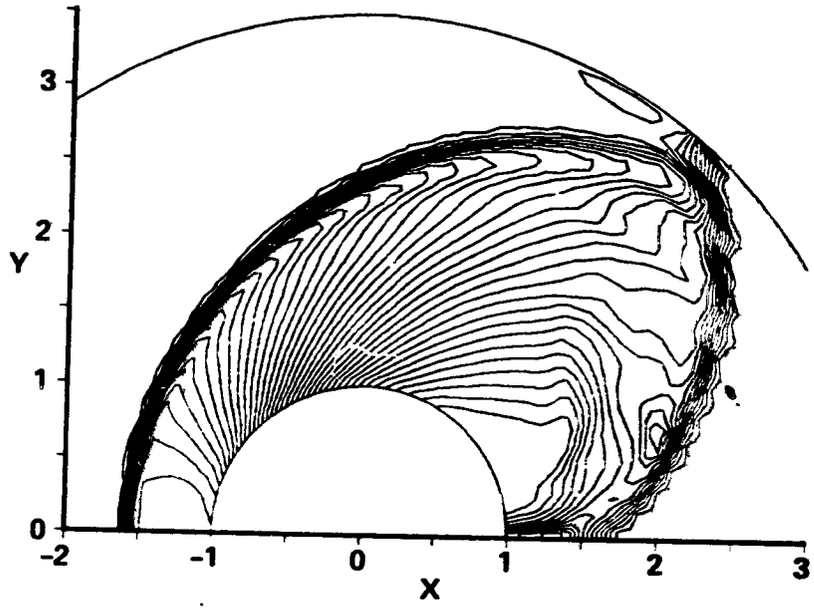

(b) Density contours: Explicit TVD method.

Fig. 4. Pressure and density contours for the shock-wave cylinder interaction. ($M_s = 10$).